



# Detection of flow units of Quseir Formation (Lower Campanian) as a potential reservoir using experimental correlations of capillary pressure derived parameters, Gebel el-Silsila, Egypt

Osama M. Elnaggar<sup>1</sup> · Mostafa G. Temraz<sup>2</sup> · Mohamed K. Khallaf<sup>3</sup>

Received: 28 January 2020 / Accepted: 28 April 2020 / Published online: 8 May 2020  
© The Author(s) 2020

## Abstract

Sandstone surface samples were collected from Quseir Fm., a member of Nubian Sandstone at Gebel el-Silsila and subjected to petrographical investigation using polarizing microscope. X-Ray diffraction was carried out to determine mineralogy. Scanning electron microscope also was utilized for the morphological characterization of the rock components. This sandstone petrofacies is mainly quartz arenite. The depositional environment of the studied sandstones is fluvial to fluvial-marine, and they suffered post-depositional alterations. Alterations include diagenesis (clay infiltration and original detrital grains disintegration), weathering, deterioration phenomena as erosion, voids existence due to dissolution and absence of bound materials. Mineralogical characterization indicated that quartz is the main constituent of sandstone in addition to kaolinite clay mineral as a cementing material. Petrophysically, the studied samples subjected to porosity and permeability measurements. The measurements showed that the samples are highly porous and permeable. Permeability–porosity relation displayed two groups (A and B). Although porosity values are close to great extent, permeability is quite different for the two groups due to the different distributions of pore throats, perhaps as a result of uneven clay distribution within the two groups of samples. Many capillary pressure-derived parameters were calculated using experimental correlations. The results confirmed the presence of two flow groups, macroport group (group A) and megaport group (group B) that is the best in terms of reservoir quality. The two groups reflect the excellent properties for the studied potential reservoir.

**Keywords** Petrography · Petrophysics · Flow zones · Quseir Formation · Gebel el-silsila

## Introduction

Gebel el-Silsila is located south Edfu and north Kom Ombo, and it is about 65 km north of Aswan [24° 38.48', 24° 39.05' N and 32° 55.75', 32° 56.04' E], (Fig. 1). It seems as elevations of Nubian Sandstone (Temraz and Khallaf 2016) on West and East Banks of the Nile River. The Nubian Sandstone was studied by many authors (Nabawy et al. 2016; Temraz and Elnaggar 2016; Sarhan and Basal 2019). Quseir

Formation represents a unit of the group previously called “Nubian Sandstone” (Hermina et al. 1989; Tawadros 2001). Quseir Formation is composed mainly of sandstones of very fine to medium grain sizes. These sandstones have sedimentary structures as cross-bedding which is tabular, occasionally planar and Late Campanian in age. The sandstone of Gebel el-Silsila was excavated for obtaining stones used in building purposes. The Nubian Sandstone sequence was deposited southwestern Egypt, where the cycles of marine regressions and transgressions and soil deposits interleaved with marine silty clay and alluvial plain sand with interbedded channel controlled its deposition. Nubian Sandstone has been studied in terms of depositional environment by many authors (Said 1962; Harms 1979; Ward and McDonald 1979; Klitzsch 1979; Bhattacharyya 1980; Mansour 1984). The typical Nubian Sandstone cycles represent continuously deltaic and fluvial changing depositional environments, Klitzsch (1984). Quartzose Nubia sandstone is a name that used by early workers close to Aswan involves

✉ Osama M. Elnaggar  
osama\_221@yahoo.com

<sup>1</sup> Production Department, Egyptian Petroleum Research Institute (EPRI), Nasr City, Cairo, Egypt

<sup>2</sup> Exploration Department, Egyptian Petroleum Research Institute (EPRI), Nasr City, Cairo, Egypt

<sup>3</sup> Conservation Department, Faculty of Archaeology, Fayoum University, Fayoum, Egypt



Fig. 1 Location map of Gebel el-Silsila

five progressive lithofacies predominated by quartzose sandstone, Van Houten and Bhattacharyya (1979), where feldspars in the lower facies are lower than 5% and reach to 15% in the higher facies in the northern limits. The Nubian Sandstone outcrops of Cretaceous age in Kuruku plateau around Lake Nasser, southern Egypt, are subdivided into four formations: Abu Aggag Fm. (the oldest), Timsah Fm., Umm Brammily Fm. and Quseir Fm. (the youngest), EGPC/CONOCO-Coral (1987). Abu Aggag Fm. extends in North–South direction as a vast belt of even beds that covers Kurkur area and also east of Aswan. It is for the most part composed of fluvial stores cross-bedded, lenticular sand bodies, ripple-laminated and channel fills.

Timsah Fm. is outcropped in the southeastern Desert and consists essentially of fluvial close shore marine and locally is eolian sandstone, fine to medium grain size, interbedded with soil and channel deposits. Umm Brammily Fm. is made mainly of fluvial sandstone, changes to marine toward north direction. Quseir Fm. covers a broad region in north of Aswan direction, where its thickness is 280 m and reaches to 425 m in north direction. Quseir Fm. is mainly littoral shale of different colors, siltstone AND flaggy sandstone that contain blended marine and crisp water gastropods. Because Quseir Fm. is fair oil and gas source in adjacent area of Al Baraka oil field, Kom Ombo basin, El Nady et al. (2018), so this work is aimed at investigating the lithofacies and available flow zones of the studied samples of Quseir Fm. as a potential reservoir in the study area, using experimental relations of capillary pressure derived parameters in addition to porosity and permeability values. The capillary pressure is an important property that used to evaluate reservoir rocks through many parameters as pore

size distribution, displacement pressure, height above water level, transition zone and also fluid saturations that rely on dimensions and the geometry of the pore space (Øren and Bakke 2003; Mousavi and Bryant 2012; Likos and Jaafar 2013; Torskaya 2014). Flow zones determination helps to know the potential reservoir capabilities and the expected production, of course with other parameters of interest.

The study area was not explored before for oil production purposes and perhaps this because it contains much of antiquities, so this work is considered an adding value in terms of reservoir evaluation to know more about the characteristics of the potential reservoir. It is possible to be allowed in future for oil exploration under certain conditions in this area, and then, this study and others become important and form a database for reservoir description or evaluation and this is another benefit would be gained from this work.

## Methodology

Fourteen surface sandstone samples represent Quseir Fm. were obtained from Gebel el-Silsila. The petrographical properties through thin sections were investigated using a polarizing microscope. The mineral composition identification was conducted using X-ray diffraction, and scanning electron microscope was used for detection the morphology of the rock compositions. For carrying out the petrophysical measurements, the studied specimens plugged into cylindrical plugs of one-inch diameter sizes, where they cleaned using methanol to remove any salt remains and dried through a drying oven. Porosity was measured using both helium porosimeter of Heise Gauge type for grain volume determination and DEB-200 apparatus for measuring bulk volume parameter. Permeability measurements were taken using air permeameter. Cross-sectional area and length of the sample, flow rate and viscosity of the used fluid and differential pressure through the tested sample are parameters used to calculate the permeability value.

## Results and discussion

### Petrography

The present petrographic examination of Gebel el-Silsila sandstone was carried out to show facies type, the principle rock constituents, cement, pores, diagenesis and depositional environment. It found out that this sandstone represents quartz arenite facies. The terminology of the examined sandstone follows Williams et al. (1982), where unclean sandstones are those contain at least 10% argillaceous materials as quartz wacke and lithic wacke, whereas clean sandstones as arenites are free from argillaceous materials.

Lowering the percent of argillaceous matter increases the degree of sandstone maturation as the feldspathic arenites, while quartz arenite represents complete mature case. The majority of the mature sandstones have more extended sedimentary history than that of the less mature rocks, where they often include cycles of erosion and deposition. Sandstones are rich in feldspar typically sourced from granitoid volcanic rocks or higher rank feldspathic gneisses or schists. The examined sandstone samples are mostly quartz arenite microfacies made of fine monocrystalline quartz grains, sub-angular, moderately sorted and cemented by authigenic kaolinite clay mineral. Sandstones always are grain-supported with point or elongate contacts and characterized by high-percent intergranular porosity as distinguished by blue color within the studied thin section. This arenite microfacies may points out to feldspathic arenite because of existence of feldspar in dissolved and fresh state. The dissolving of feldspar caused development of pore filling kaolinite clay mineral which may affect negatively the rock porosity and permeability to some degree (Fig. 2a, b). This arenite is considered a mature microfacies due to its mineralogy and texture. The existence of altered and fresh feldspars (Fig. 3a, b), subangular grains and high maturity nature, demonstrates that this sandstone obtained from granitoid high-grade feldspathic gneisses/schists or igneous rocks. The depositional condition of this microfacies may be fluvial environment due to the existence of straight and curved grooves on the quartz grain surfaces (Fig. 3b).

## XRD

XRD analysis of bulk mineral composition of sandstone samples (Fig. 4a, b) displays that they composed mainly of quartz ( $\text{SiO}_2$ ) with traces of kaolinite  $\text{Al}_2\text{Si}_2\text{O}_5(\text{OH})_4$  and orthoclase  $\text{K}(\text{Al,Fe})\text{Si}_2\text{O}_8$ .

## Petrophysics

Petrographical description shows that all the studied samples are related to one lithofacies, but at the same time, two different petrophysical units can be differentiated (A and B), and this is shown through permeability–porosity correlation that displayed with sample numbers, (Fig. 5a). The values of porosity and permeability of the studied samples reflect very good reservoir properties, Levorsen (1967).

Porosity and permeability can be used to characterize the reservoir quality to great extent, and many authors studied the relation between them (Tiab and Donaldson 2004; Díaz-Viera 2006; Erdely and Díaz-Viera 2009; Nabawy and Al-Azazi 2015). The parameter  $\sqrt{k/\phi}$  (pore geometry factor) was selected to express the two previous properties together for plotting with other different petrophysical parameters for estimating the studied samples (Fig. 6a, b). Petrophysical

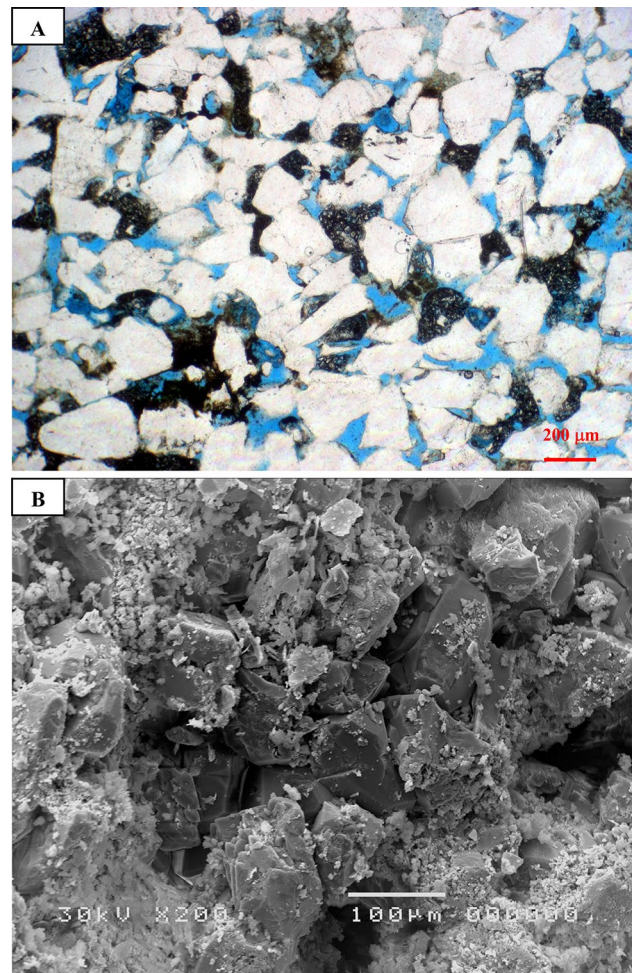


**Fig. 2** Photomicrograph of high-porosity quartz arenite, S#3, group (B),  $\phi = 29.3\%$ ,  $K = 3578\text{mD}$ . **a** PPL, **b** SEM

evaluation for the studied samples was achieved using experimental correlations to calculate different reservoir parameters utilizing the results of porosity and permeability. These are  $r_{35}$ ,  $r_{\text{thresh}}$ ,  $r_{\text{apex}}$  and reservoir quality index (RQI). The first one is  $r_{35}$  and calculated using the equation of Winland, Kolodzie (1980).

$$\log r_{35} = 0.732 + 0.588 \log k_{\text{air}} - 0.864 \log \phi \quad (1)$$

where  $r_{35}$  = the pore radius equivalent to 35% saturation of mercury.  $K_{\text{air}}$  = sample permeability (mD).  $\phi$  = sample porosity (%).

Winland displayed in field examples that  $r_{35}$  can be applied to describe stratigraphic traps of economical hydrocarbon accumulations. The previous conclusion confirmed by Pittman (1989), where  $r_{35}$  higher than  $0.5 \mu\text{m}$  used to delineate the trap. According to Martin et al. (1997), and based on  $r_{35}$  values, the studied samples were separated into two groups (Fig. 5b) based on Winland lines using his equation, where

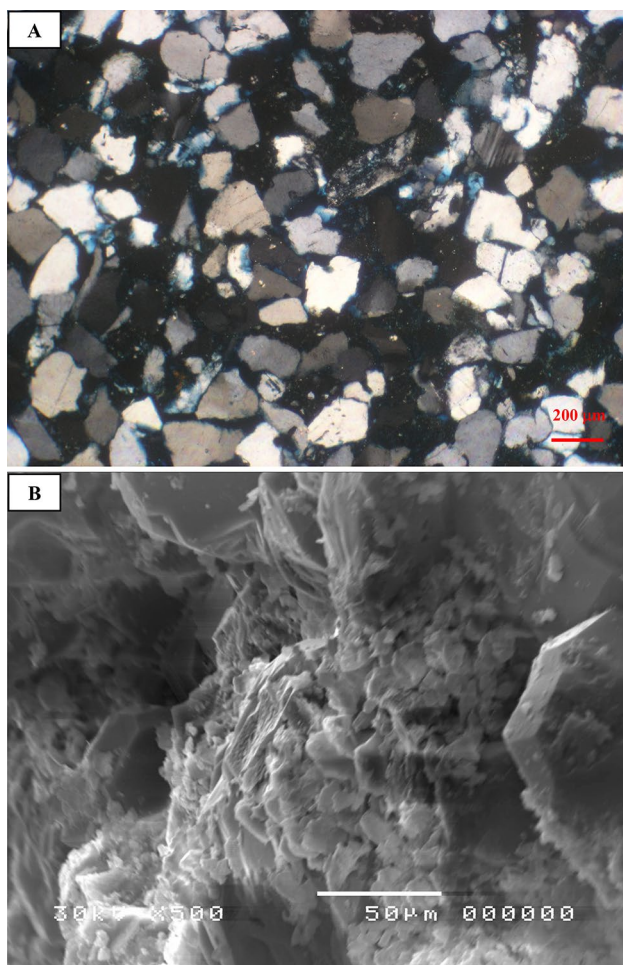


**Fig. 3** Photomicrograph of high-porosity quartz arenite with fresh and altered feldspar, S#15, group (A),  $\phi=28.8\%$ ,  $K=257\text{mD}$ . **a** CN, **b** SEM

macroport flow unit samples (group A) lie below 10- $\mu\text{m}$  line and megaport flow unit samples (group B) lie above 10- $\mu\text{m}$  line; hence,  $r_{35}$  tell us that group (B) has great potentiality for fluids production/injection relative to that of group (A).

Although Winland did not point out the reason that  $r_{35}$  gave the best correlation in his work, Pittman (1992), mentioned, this perhaps due to at this radius, the pore network is evolved to an effective pore system which dominates flow as described by Swanson (1981). Another petrophysical parameter that calculated according to Pittman (1992) is the pore aperture radius ( $r_{\text{thresh}}$ ) that refers to the threshold pressure and determined by ( ). It is the pressure at which mercury builds connected way through the sample.

$$\log r_{\text{thresh}} = 0.137 + 0.479 \log k_{\text{air}} - 0.143 \log \phi \quad (2)$$

where  $r_{\text{thresh}}$  = the pore radius equivalent to a threshold pressure,  $\mu\text{m}$ .  $K_{\text{air}}$  = sample permeability (mD).  $\phi$  = sample porosity (%).

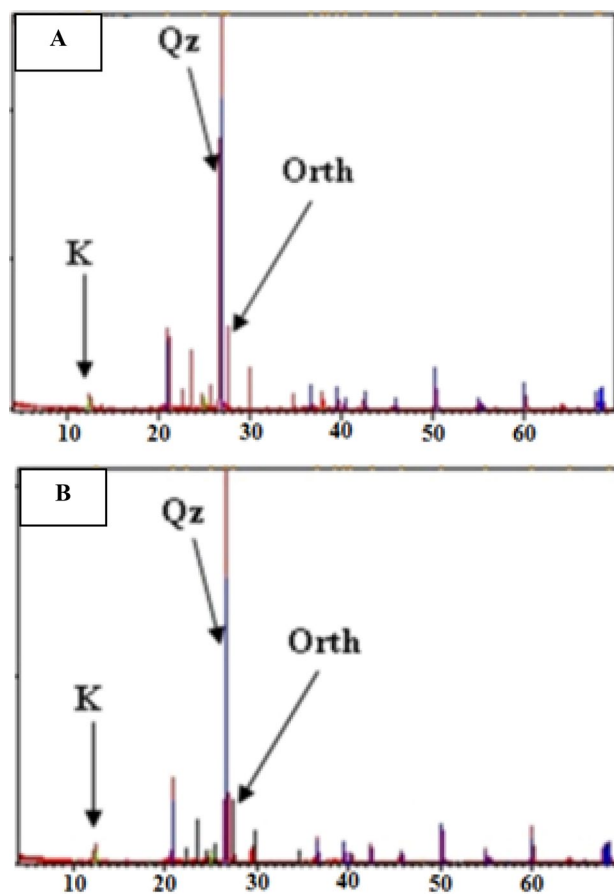


**Fig. 4** XRD graph displays bulk mineral composition of sandstone samples. **a** S#8, group (A),  $\phi=29.9\%$ ,  $K=149\text{mD}$ . **b**: S#3, group (B),  $\phi=29.3\%$ ,  $K=3578\text{ mD}$

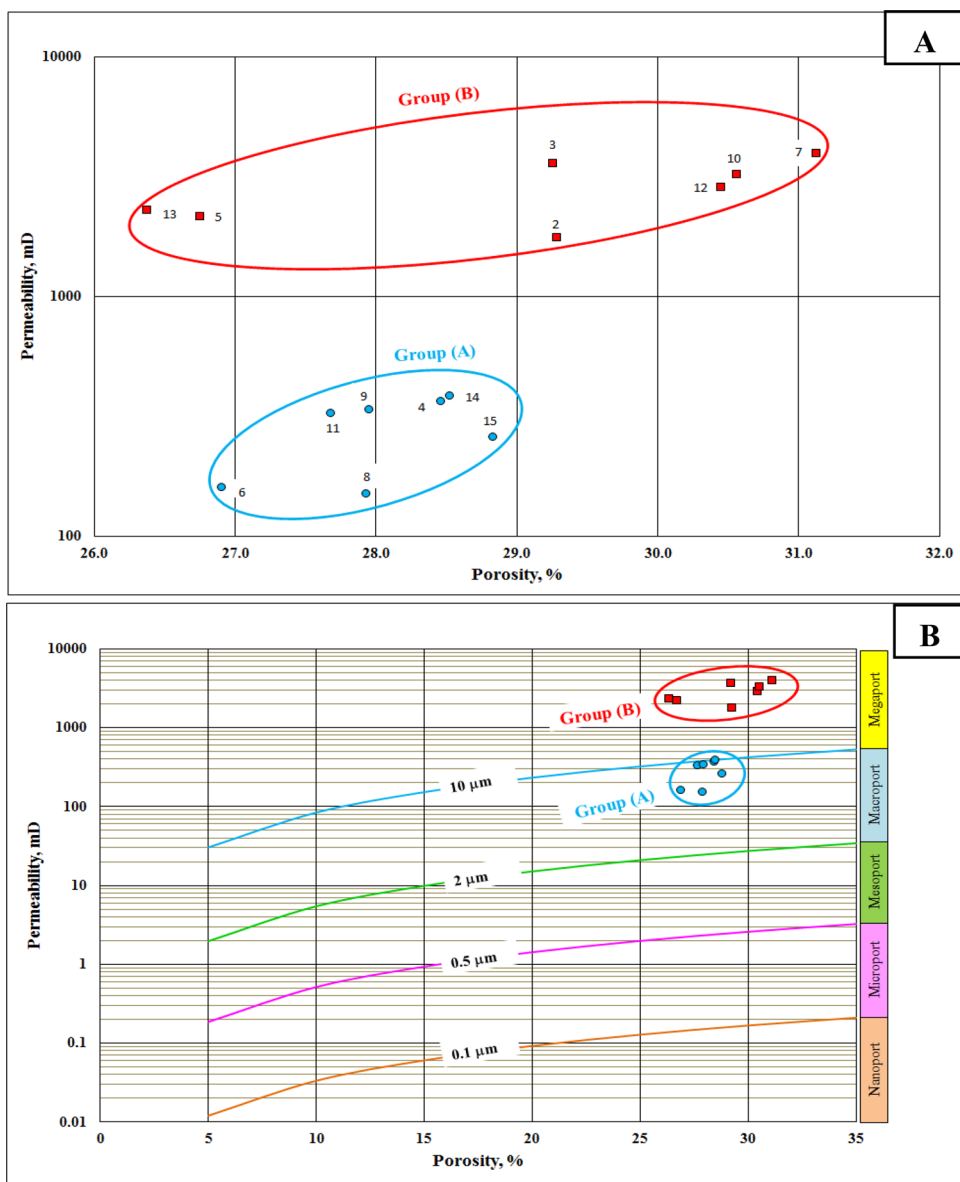
The results of ( $r_{\text{thresh}}$ ) displayed that samples of group (B) have higher values of ( $r_{\text{thresh}}$ ) relative to those of group (A), and (Fig. 6a), this confirms the high-quality properties of group (B) samples. An important reservoir parameter is determined by Swanson (1977), where he determined the position of the point on the mercury injection curve which clarifies a well-interconnected pore system across the rock, where this point refers to apex of the hyperbola of a log–log plot of capillary pressure and bulk volume mercury saturation by Swanson (1981); hence, pore radius ( $r_{\text{apex}}$ ) that corresponds to apex was calculated as follows according to Pittman (1992), (Fig. 6a):

$$\log r_{\text{apex}} = -0.117 + 0.475 \log k_{\text{air}} - 0.099 \log \phi \quad (3)$$

where  $r_{\text{apex}}$  = the pore radius apex of hyperbola of a log–log plot on the mercury injection curve.  $K_{\text{air}}$  = air permeability (mD).  $\phi$  = porosity (%).

The results of ( $r_{\text{apex}}$ ) showed that (Fig. 6a) samples of the group (B) have higher ( $r_{\text{apex}}$ ) values relative to those of group (A), and this is agreed with ( $r_{\text{thresh}}$ ) results and

**Fig. 5 a** Permeability (mD) versus porosity (%) **b** flow units differentiation using Winland flow lines

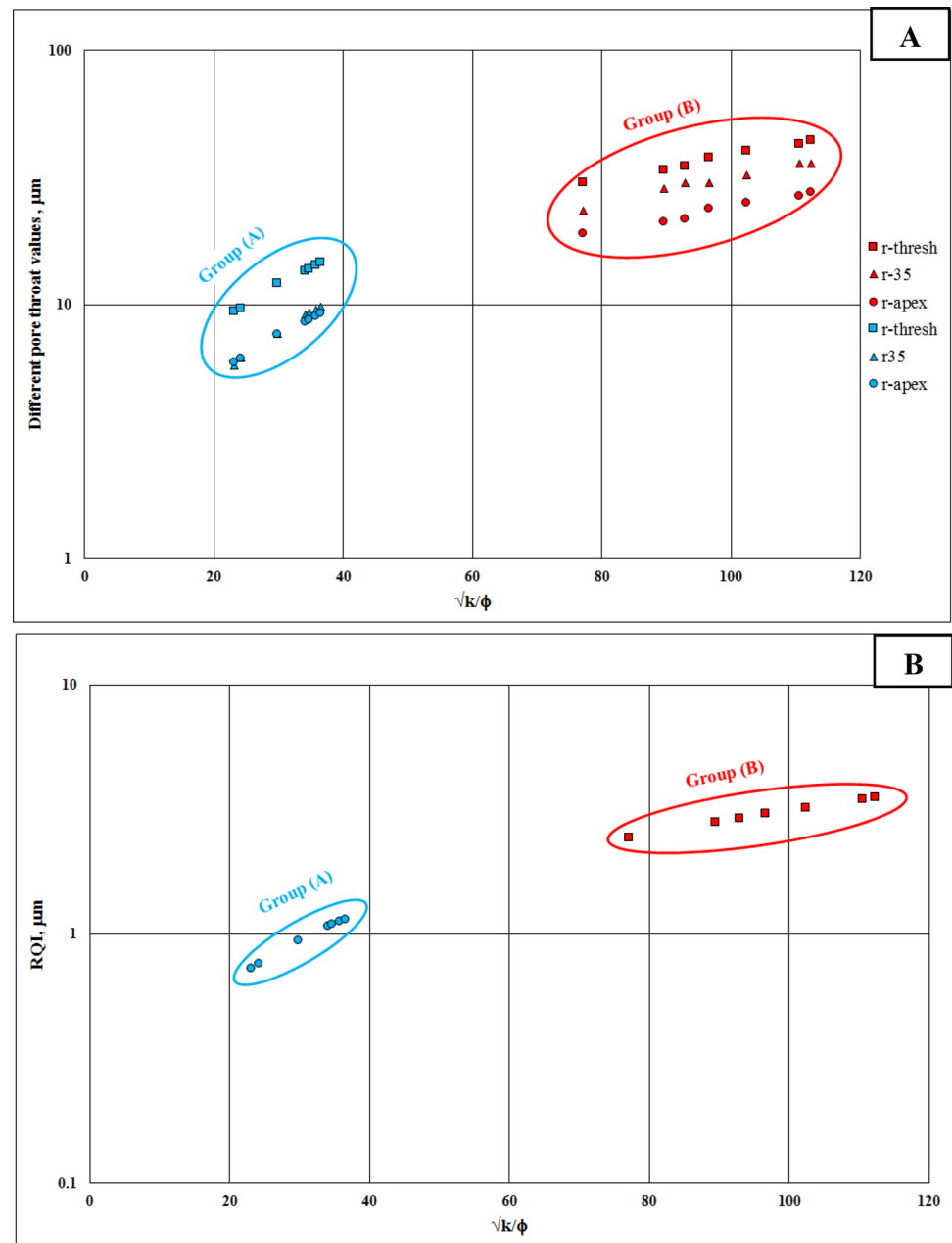


confirms that the best rock quality is for group (B) samples. Also  $r_{35}$  is displayed again (Fig. 6a), to show the consistence between different pore throat concepts, where the higher values of  $r_{35}$  exist within group (B). The last rock parameter determined for the studied samples is RQI or reservoir quality index. This parameter was used (Amaefule et al. 1993) with the normalized porosity to separate the different flow units existing within a rock, where group (B) has the best RQI values (Fig. 6b).

All the results confirmed that the samples of the group (B) are better than those of group (A) in terms of reservoir properties, and this means that group (B) represents the best flow properties and hence the best performance for a the potential oil productive reservoir. Actually, pore throat size distribution is an important factor responsible for giving a reservoir its own capillary pressure, quality

and performance. Although the two groups have very close porosity values, they have different pore throat size distributions. This difference leads to different capillary pressures characterizing the accompanying flow zones. The wide spaces pore size distribution has low capillary pressure and is characterized by largest pore throats, which means a permeable flow unit capable of producing petroleum or infiltrating injection fluids in an easy way that will affect positively oil recovery and the reverse is right in case of the narrow spaces pore size distribution. Thin sections photomicrograph (Fig. 7a, b) represents the two flow groups, where sample#8 of group (A) has the permeability equals 149 mD and sample#3 of group (B) has the permeability equals 3578 mD, although there is only 1.4% difference between them in porosity values. Figure 7b displays that sample#3 of group (B) has the widest pore spaces network characterized

**Fig. 6** **a** Different pore throat values ( $\mu\text{m}$ ) versus  $\sqrt{k/\phi}$  **b** RQI versus  $\sqrt{k/\phi}$



by largest pore throats comparing with those of sample#8 of group (A) (Fig. 7a). The different pore space networks were a strong factor behind the differentiation of the studied samples of Quseir Fm. into macroport and megaport flow units according to  $r_{35}$  values. The macroport flow unit has the narrower pore spaces network, as a result the relatively higher the capillary pressures hence the lower the values of permeability,  $r_{35}$ ,  $r_{\text{thresh}}$ ,  $r_{\text{apex}}$  and RQI. The reverse is right in case of megaport flow unit that has the wider pore spaces

system, and consequently, the lower the capillary pressures and the higher the values of permeability,  $r_{35}$ ,  $r_{\text{thresh}}$ ,  $r_{\text{apex}}$  and RQI. The values of  $r_{35}$  tell us that Quseir Fm. as a potential reservoir would be able to produce tens of thousands and thousands of barrels of oil per day from megaport and macroport flow units, respectively, Martin et al. (1997). All petrophysical properties of the studied samples are displayed (Table 1), where the samples are arranged according to permeability increasing.

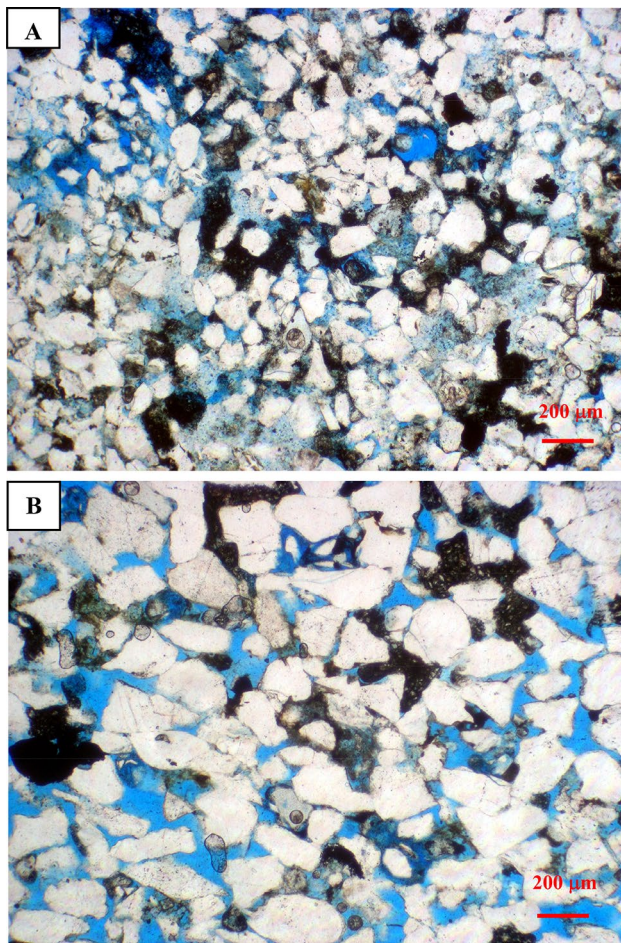


**Fig. 7** Photomicrograph (PPL) of high-porosity quartz arenite. **a** S#8 represents group (A),  $K=149$  mD &  $\phi=27.9\%$ . **b** S#3 represents group (B),  $K=3578$  mD &  $\phi=29.3\%$

## Conclusion

Surface sandstone samples of Quseir Fm. were collected from Gebel el-Silsila and subjected to petrographical and petrophysical investigation. The studied sandstones represent quartz arenite microfacies (feldspathic). The depositional environment of the studied sandstones is fluvial-marine to fluvial. The samples suffered post-depositional alteration as diagenesis (clay infiltration and original detrital grains disintegration), weathering, deterioration phenomena as erosion and voids existence due to dissolution and absence of bound materials. The mineralogical description indicated that quartz is the main constituent of sandstone in addition to kaolinite clay mineral as a cementing material. Petrophysical investigation showed that all the studied samples are porous and permeable but can be separated into two groups (A and B). The samples of two groups have close porosity values to great extent but with obvious different permeability values. The samples differentiation into macroport (group A) and megaport (group B) flow units is attributed to the dissimilar distribution of pore throats, perhaps as a result of uneven clay distribution within the two groups of samples. Different petrophysical parameters confirmed that Quseir Fm. has different flow properties where pore throat size distribution for group (B) is better than that of group (A). The best flow properties of group (B) reflect the best performance for the reservoir of interest in case of being oil productive. Someday, if the petroleum explorations in the studied area proved that the presence of complete oil system in terms of source rocks, traps and cap rocks, in addition to an enough

**Table 1** Petrophysical properties of the studied samples

Flow units	Sample	Porosity %	K mD	$(k/\phi)^{0.5}$	$r_{\text{apex}}$ $\mu\text{m}$	$r_{35}$ $\mu\text{m}$	RQI $\mu\text{m}$	$r_{\text{thresh}}$ $\mu\text{m}$
Macroport group (A)	8	27.9	149	23.12	5.92	5.77	0.726	9.36
	6	26.9	158	24.25	6.11	6.16	0.761	9.68
	15	28.8	257	29.87	7.64	7.72	0.938	12.10
	11	27.7	323	34.17	8.56	9.15	1.073	13.58
	9	28.0	337	34.71	8.72	9.30	1.090	13.83
	4	28.5	365	35.79	9.03	9.59	1.124	14.33
	14	28.5	382	36.60	9.24	9.84	1.149	14.65
	Megaport group (B)	2	29.3	1746	77.22	18.96	23.50	2.425
5		26.8	2147	89.59	21.10	28.70	2.813	33.80
13		26.4	2277	92.92	21.73	30.08	2.918	34.83
12		30.5	2846	96.67	23.82	30.28	3.035	37.97
10		30.6	3206	102.41	25.19	32.38	3.216	40.17
3		29.3	3578	110.58	26.66	35.87	3.472	42.61
7		31.1	3932	112.39	27.71	35.94	3.529	44.19

thickness and lateral extension for the oil carrier beds, while megaport flow units are prevailing, then a high oil productivity would be expected from Quseir Fm.

**Open Access** This article is licensed under a Creative Commons Attribution 4.0 International License, which permits use, sharing, adaptation, distribution and reproduction in any medium or format, as long as you give appropriate credit to the original author(s) and the source, provide a link to the Creative Commons licence, and indicate if changes were made. The images or other third party material in this article are included in the article's Creative Commons licence, unless indicated otherwise in a credit line to the material. If material is not included in the article's Creative Commons licence and your intended use is not permitted by statutory regulation or exceeds the permitted use, you will need to obtain permission directly from the copyright holder. To view a copy of this licence, visit <http://creativecommons.org/licenses/by/4.0/>.

## References

- Amaefule JO, Altunbay M, Tiab D, Kersey D, Keelan DK (1993) Enhanced reservoir description: using core and log data to identify hydraulic (flow) units and predict permeability in uncored intervals/wells. In: 66th annual SPE conference and exhibitions held in Houston, Texas, Oct 3–6
- Bhattacharyya DP (1980) Sedimentology of the late cretaceous Nubia formation at Aswan, southeast Egypt, and origin of the associated ironstones [Ph.D. thesis]. Princeton, New Jersey, Princeton University, p 122
- Díaz-Viera M, Anguiano-Rojas P, Mousatov A, Kazatchenko E, Markov M (2006) Stochastic modeling of permeability in double porosity carbonates applying a Monte-Carlo simulation method with t-copula. In: SPWLA 47th annual logging symposium
- EGPC, CONOCO-Coral (1987) Geological Map of Egypt, Scale 1:500,000. EGPC, Cairo
- El Nady MM, Ramadan FS, Hammada MM, Mousa DA, Lotfy NM (2018) Hydrocarbon potentiality and thermal maturity of the Cretaceous rocks in Al Baraka oil field, Kom Ombo basin, south Egypt. *Egypt J Pet* 27(4):1131–1143
- Erdely A, Díaz-Viera M (2009) Nonparametric and semiparametric bivariate modeling of petrophysical porosity-permeability well log data. Lecture Notes in Statistics. In: Jaworski P et al (eds) Copula theory and its applications. 198, 267–278. Springer, Berlin
- Harms JC (1979) Alluvial-plain sediments of Nubia Southwestern Egypt. *AAPG Bull* 63(5):829
- Hermína M, Klitzsch E, List FK (1989) Stratigraphic lexicon and explanatory notes to the Geological map of Egypt 1: 500.000. Cairo: Conoco Inc
- Katz AJ, Thompson AH (1986) Quantitative prediction of permeability in porous rock. *Phys Rev B* 34:8179–8181
- Katz AJ, Thompson AH (1987) Prediction of rock electrical conductivity from mercury injection measurements. *J Geophys Res* 92:599–607
- Klitzsch E (1984) Northwestern Sudan and bordering areas; geological development since Cambrian time *Berliner GeowissAbh* 50 (A): 23–45
- Klitzsch E, Harms JC, Lejal-Nicol A, List FK (1979) Major subdivisions and depositional environments of Nubia strata, southwestern Egypt. *AAPG Bull* 63(6):967–974
- Kolodzie SJr (1980) Analysis of pore throat size and use of the Waxman-Smits equation to determine OOIP in Spindle field, Colorado. In: SPE, 55th annual fall technical conference, paper SPE-9382, p 10
- Levorsen AL (1967) *Geology of petroleum*, 2nd edn. Freeman, San Francisco, p 724
- Likos WJ, Jaafar R (2013) Pore-scale model for water retention and fluid partitioning of partially saturated granular soil. *J Geotech Geoenviron Eng* 139(5):724–737
- Mansour AAM (1984) Sedimentological studies on the Nubian sandstone, Eastern Desert. M.Sc. Thesis, Faculty of Science. Assiut University, Egypt, p 255
- Martin AJ, Solomon ST, Hartmann DJ (1997) Characterization of petrophysical flow units in carbonate reservoirs. *AAPG Bull* 81(5):734–759
- Mousavi MA, Bryant SL (2012) Connectivity of pore space as a control on two-phase flow properties of tight-gas sandstones. *Transp Porous Med* 94(2):537–554
- Nabawy BS, Al-Azazi NAS (2015) Reservoir zonation and discrimination using the routine core analyses data: the upper Jurassic Sab'atayn sandstones as a case study, Sab'atayn basin Yemen. *Arab J Geosci* 8(8):5511–5530
- Nabawy BS, Geraud Y (2016) Impacts of pore- and petro-fabrics, mineral composition and diagenetic history on the bulk thermal conductivity of sandstones. *J Afr Earth Sci* 115:48–62
- Øren P, Bakke S (2003) Reconstruction of berea sandstone and pore-scale modelling of wettability effects. *J Petrol Sci Eng* 39(3):177–199
- Pittman ED (1989) Nature of the Terry sandstone reservoir, Spindle field, Colorado. In: Coalson EB (ed) *Petrogenesis and petrophysics of selected sandstone reservoirs of the rocky mountain region*. Denver, CO, RMAG, pp 245–254
- Pittman ED (1992) Relationship of porosity and permeability to various parameters derived from mercury injection-capillary pressure curves for sandstone. *AAPG Bull* 76(2):191–198
- Said R (1962) *The geology of Egypt*. Elsevier, Amsterdam, p 377
- Sarhan MA, Basal AMK (2019) Evaluation of Nubia sandstone reservoir as inferred from well logging data interpretation for Rabeh East-25 well, Southwest Gulf of suez Egypt. *J Afr Earth Sci* 155(7):124–136
- Swanson BF (1977) Visualizing pores and non-wetting phase in porous rocks. In: SPE, annual fall technical conference, SPE 6857 10
- Swanson BF (1981) A simple correlation between permeabilities and mercury capillary pressures. *J Pet Technol* 33(12):2488–2504
- Tawadros EE (2001) *Geology of Egypt and Libya*. AA Balkema, Rotterdam 1–468 [A. Miller/A. Hendy/M. Carrano]
- Temraz MG, Elnaggar OM (2016) Nubian Sandstone reservoir characteristics: sedimentological and petrophysical evaluation in the Southern Gulf of Suez Egypt. *Appl Earth Sci (Trans Inst Min Metall B)* 125(2):63–72
- Temraz MG, Khallaf MK (2016) Weathering behavior investigations and treatment of Kom Ombo temple sandstone, Egypt—based on their sedimentological and petrographical information. *J Afr Earth Sci* 113:194–204
- Tiab D, Donaldson EC (2004) *Petrophysics: theory and practice of measuring reservoir rock and fluid transport properties*. Gulf Professional Publishing is an imprint of Elsevier, 200 Wheeler Road, Burlington, MA 01803, USA, 880. Linacre House, Jordan Hill, Oxford OX2 8DP, UK
- Torskaya T, Shabro V, Torres-Verdín C, Salazar-Tio R, Revil A (2014) Grain shape effects on permeability, formation factor, and capillary pressure from pore-scale modeling. *Transp Porous Med* 102(1):71–90
- Van Houten FB, Bhattacharyya DP (1979) Late cretaceous Nubia formation at Aswan southeastern desert Egypt. *Annals of Geological survey, Egypt IX*, pp 408–431
- Ward WC, McDonald KC (1979) Nubia Formation of central Eastern Desert, Egypt—Major subdivisions and depositional setting. *AAPG Bull* 63:975–983



Williams H, Turner FJ, Gilbert C (1982) Petrography, an introduction to the study of rocks in thin sections, 2nd edn. W.H. Freeman Company Inc., San Francisco, p 626

**Publisher's Note** Springer Nature remains neutral with regard to jurisdictional claims in published maps and institutional affiliations.